Outward sodium current in beating heart cells

David P. Wellis, Louis J. DeFelice, and Michele Mazzanti
Department of Anatomy and Cell Biology, Emory University School of Medicine, Atlanta, Georgia 30322

ABSTRACT This article is a study of the fast Na current during action potentials. We have investigated the outward Na current (Mazzanti, M., and L. J. DeFelice. 1987. *Biophys. J.* 52:95–100) in more detail, and we have asked whether it goes through the same channels associated with the rapid depolarization phase of action potentials. We address the question by patch clamping single, spontaneously beating, embryonic chick ventricle cells, using two electrodes to record the action potential and the patch current simultaneously. The chief limitation is the capacitive current, and in this article we describe a new method to subtract it. Varying the potential and the Na concentration in the patch pipette, and fitting the corrected currents to a standard model (Ebihara, L., and E. A. Johnson. 1980. *Biophys. J.* 32:779–790), provides evidence that the outward current is carried by the same channels that conduct the inward current. We compare the currents in beating cells to currents in nonbeating cells using whole-cell and cell-attached patch clamp recordings. The latter tend to show more positive Na reversal potentials, with the implication that internal Na is higher in beating cells. We propose that the plateau of the action potential, which is partly due to an inward Ca current, exceeds Na action current reversal potentials, and that this driving force gives rise to an outward movement of Na ions. The existence of such a current would imply that the fast repolarization phase after the upstroke of cardiac action potentials is partly due to the Na action current.

INTRODUCTION

The patch-clamp technique makes it possible to study the kinetics, conductance, and reversal potential of the fast Na current during the spontaneous beat of heart cells. The procedure assumes that the time average of events in the patch is equivalent to the ensemble average of similar events in the cell. We have previously shown that Na models based on voltage-clamp experiments account for the qualitative features of the cardiac Na action current (Mazzanti and DeFelice, 1987). The unique feature of free-running, spontaneously beating cells is that the Na reversal potential is ~25 mV less positive than in nonbeating cells, thus the potential at which Na reverses can be below the action potential at some point, resulting in an outward movement of Na ions.

An outward Na current would cause an early and rapid repolarization phase of the action potential. A sharp spike at the beginning of action potentials is a common feature of many cardiac cells, but it is usually attributed to the K-conducting, early-outward channel, not the fast Na channels. Our results imply that beating elevates internal Na, at least during some phases of the cycle. Movement of Na out of the cell by this mechanism would impose different requirements for the Na-K pump in beating versus nonbeating cells.

Because the dynamic Na current coincides with the capacitive current during the upstroke, subtracting the capacitive transient caused by the upstroke is crucial to our technique. In a previous study, we calculated (dV/dt) from the action potential and subtracted $c(dV/dt)$ from the patch current; c was found by equating (dV/dt) to the peak of the measured current (Mazzanti and DeFelice, 1987). Because the inward Na current reduces the peak of the outward capacitive transient, our previous method is inherently wrong. This paper reports a new method of calculating the capacitive current from a region of the data that does not include i_{NA}. To further improve the subtraction, we included a linear leak conductance in the background current. By selecting patches with extremely high seal resistances, the leak error is practically negligible. To help identify the current as Na, we varied the tip potential and the Na concentration in the patch pipette. We also compared the results with the Ebihara and Johnson (1980) model for Na current in heart. The qualitative conclusions are the same as in our previous work, but we are now able to give better estimates of the Na reversal potential and the fraction of Na that flows out of the cell.

METHODS

Tissue culture and solutions

Embryonic ventricle cells were prepared by enzymatic digestion of 7-d-old chick embryo hearts, following the procedure of DeHaan (1967)

0006-3495/90/01/41/08 $2.00

as recently revised by Fujii et al. (1988). After 12–24 h in tissue culture medium, we washed the isolated cells with the standard bath solution just before the experiments. All the experiments were done at room temperature. The composition of the bath solution (in millimolar) was: 130 Na, 1.3 K, 1.5 Ca, 0.5 Mg, 133 Cl, 0.5 SO_4, 1.3 PO_4, 5 dextrose, 10 Hepes, pH 7.35. The pipette solution similar to the bath solution except that it contained 3 mM Co and either 20 Na/110 TEA, 60 Na/70 TEA, or 120 Na/10 TEA; also Cl replaced SO_4 and PO_4. The whole-cell electrode contained an intracellularlike solution consisting of 120 K, 0.1 Ca, 2 Mg, 122.2 Cl, 1.1 EGTA, 10 Hepes, pH 7.35. Under these conditions about half the cells beat spontaneously, however, the rate is highly variable, and beating cells may stop or change their rate spontaneously when patched. We selected cells beating at a rate between about 0.8 and 1.2 times per second.

Electrodes and recording techniques

The electrodes were made from borosilicate glass (No. 7052, Corning Glass Works, Corning, NY) using a programmable puller (Sachs-Flaming, PC-84, Sutter Instrument Co., San Rafael, CA). Before pulling, we keep the glass at 470°C for at least 24 h. This procedure cleans the surface of the glass and gives the electrodes more uniform shapes with the same program. We coat the tips with Sylgard (Dow Corning Corp., Midland, MI) and store the electrodes in a dry vacuum oven at 100°C for an indefinite period. The tips were fire-polished to 1–2 μm outside diameter just before using them. The filled pipettes had resistances of 4–10 megohms when dipped into the bath solution. The estimated surface area of the patch formed with these electrodes is between 5 and 7 μm^2 by geometric and capacitive measurements (Kell and DeFelice, 1988; Mazzanti and DeFelice, 1987). The current and voltage electrodes were 5–15 μm apart on the surface of the cell. The action potentials we measure using whole-cell electrodes or 3 M KCl microelectrodes are virtually the same. The mechanical beat of the cell, which we observe during the experiment, does not change appreciably after breaking the patch in the whole-cell recording electrode, and beating continues under these conditions without apparent change (beyond that which is within the normal range for single cells) for up to 1 h, in spite of the low Ca and low Na in the whole-cell electrode solution. We interpret this as meaning that beating cells control their own internal environment. Before doing a complete analysis, we identified patches that contained Na channels by applying a positive potential to the cell-attached electrode. This hyperpolarizing potential revealed a large inward current just at the upstroke of the action potential only if the patch contains Na channels. This large inward current was never present in patches containing 10^{-6} M TTX, however, a small TTX-insensitive current always appears to be present. The kinetics of the action current agree qualitatively with standard Na channel models, and this correspondence was used to help identify the current as Na (Mazzanti and DeFelice, 1987). In the present paper we also vary patch Na concentration and patch potential.

We used List EPC5 and EPC7 amplifiers (Medical Systems Corp., Greenville, NY) to measure the voltage and current and a VCR (Panasonic Co., Secaucus, NJ) to store the data. We analyzed the data on a model 4094 oscilloscope (Nicolet Instrument Corp., Madison, WI) and an AT computer (IBM Corp., Danbury, CT). For more details on the dual-electrode recording technique see Mazzanti and DeFelice (1987, 1988). Note, however, that the present article uses a new method to subtract the background and capacitive current, which we refer to below as the error current.

TABLE 1 Estimated values of c, g, i_o, and sum of standard errors resulting from all calculations of error current from 20 two-electrode experiments on eight cells

	c	g	i_o	SSE
	pF	*pS*	*pA*	
Mean	0.2418	1.268	0.0310	15.02
Range	0.0979–0.3356	0.0632–3.783	−0.4426–0.5857	6.530–27.11

Pipette Na concentration varied from 20 to 120 mM Na and applied pipette potential (V_p) ranged from −20 to 40 mV.

Subtraction of the error current

The following is an outline of the procedure we use here to subtract leak and capacitive currents to estimate Na currents: (*a*) Collect 400 ms of $i(t)$ and $V(t)$ simultaneously at a 5-kHz sample rate. (*b*) Average $i(t)$ and $V(t)$ over at least 20 beats. (*c*) Truncate $\langle i(t)\rangle$, and similarly $\langle V(t)\rangle$, to exclude the Na current (see Fig. 2). (*d*) Use the truncated data to find c, g, and i_o with the formula: $\langle i(t)\rangle = c[\mathrm{d}\langle V(t)\rangle/\mathrm{d}t] + g\langle V(t)\rangle + i_o$. (*e*) Calculate an error current, $i_E(t)$, in the excluded region using the values of c, g, and i_o. (*f*) Subtract $i_E(t)$ from $\langle i(t)\rangle$ in the excluded region to obtain the first estimate of i_{NA}. (*g*) Repeat steps *c*–*e* but now truncate after the first estimate of i_{NA} returns to zero. This step gives the final estimates of c, g, and i_o. (*h*) Recollect 50 ms of $V(t)$ and $i(t)$ at 100 kHz in the excluded region. (*i*) Average these over at least 20 beats and use the final estimates of c, g, and i_o from step *g* to calculate a final $i_E(t)$ in the excluded region. (*j*) Subtract $i_E(t)$ obtained in step *i* from the measured $i(t)$ for the final estimate of i_{NA}.

Marquardt's nonlinear, least squares, regressive curve-fitting routine was used to calculate the values of c, g, and i_o that most closely fit the data (see Fig. 2 for examples). Table 1 summarizes the final estimates of c, g, and i_o obtained from all experiments. If c were due entirely to the patch, we would expect 0.07 pF from the 7 μm^2 surface area formed by the omega figure drawn into the pipette (Sakmann and Neher, 1983, p. 45). Mazzanti and DeFelice (1987) showed that coupling between electrodes accounts for most of the measured capacitance, and that the lower limit of ~0.07 pF is only achieved in one-electrode experiments. We approached this lower limit in some two-electrode experiments and attribute the range of c to variable interelectrode spacing rather than patch area. We selected patches in which g was extremely low. This conductance, which in the worst case corresponds to 250 gigohms, is not due to resolvable channels that open and close during the action potential, but rather to a constant, residual leak. This method of leak subtraction does not exclude the possibility that a Na window current contributes to g. If we perform the subtraction by truncating at 30 or 250 ms after the upstroke, we get the same values for all the parameters (Fig. 2). The Na window current in this experiment is at most a constant 0.6 pS, and we are reducing our estimate of Na conductance by this constant value. The offset current, i_o, is primarily caused by the hyperpolarizing and depolarizing voltages we applied to the patch, which accounts for the wide and nearly symmetric range of this parameter.

We plot i_{NA} as a function of the time during the action potential, $i_{NA}(t)$, and as a function of the voltage during the action potential, $i_{NA}(V)$. The time integral of $i_{NA}(t)$,

$$\int \langle i_{NA}(t)\rangle \mathrm{d}t,$$

is a measure of the amount of Na that flows in and out the patch under the different conditions of our experiments. With 120 mM Na in the pipette, we hyperpolarize and depolarize the patch by clamping the pipette potential, V_p, so that channels in the patch experience either $V(t)$ or $V(t) \pm V_p$ while the rest of the cell is beating normally. For V_p =

0 we did experiments in pipette solutions containing 20, 60, and 120 mM Na.

RESULTS

Fig. 1 is a comparison of the current-voltage relationships from three experiments that promote Na currents. Fig. 1 *a* is a standard whole-cell voltage clamp of a single 7-d-old chick ventricle cell isolated in tissue culture. The inset shows examples of the current responses to voltage steps. The $I(V)$ curve is a plot of the peak currents against the test voltages. In this experiment, the bath solution contained 120 mM Na plus Ca channel and K channel blockers (see Methods). The reversal potential of the Na current is 60 mV, close to the value found for this same tissue in another study (Fujii et al., 1988). Fig. 1 *b* is a cell-attached patch recording from a nonbeating cell. At 7 d these cells are in a transition stage of development and only about half beat spontaneously. Applying depolarizing steps to the patch, which contains the same solution as the bath in Fig. 1 *a*, revealed single Na channel currents (inset). By breaking the patch after the experiment, we were able to determine the resting potential of the cell and calculate the absolute voltage of the patch membrane. The inset shows the single-channel currents at three voltages, and the $i(V)$ curve plots the amplitude of these currents versus the absolute potential. The conductances of the two lines, which are drawn by eye and are ~9 and 15 pS, most likely represent single and double openings of channels from the same population rather than low and high conductance states or two populations of channels (Scanley and Fozzard, 1987; Patlak, 1985). Regardless, the reversal potential of 40–45 mV, although lower than the whole-cell reversal potential, is much higher than the reversal potential in beating cells (Figs. 6 and 7). Before arriving at this conclusion we must first subtract the capacitive current.

Fig. 1, *c* and *d*, are data from a similar cell, except that the cell is beating spontaneously. We record the action potential and the cell-attached patch current at the same time. Fig. 1 *c* shows the upstroke of the action potential (top) on an expanded time scale; the patch current (below) contains an outward capacitive transient interrupted midway by an inward Na current. The tip potential in the patch is 20 mV to enhance the Na current (Mazzanti and DeFelice, 1987). A plot of voltage versus current, beginning from a point just beyond the sharp reversal in the current trace, is given in Fig. 1 *d*. An outward current exists, but it is difficult to measure it accurately or assign it to Na because of the presence of the capacitive current. Fig. 2 describes our method of eliminating capacitive currents and leakage currents from the traces.

To subtract the capacitive current and leak currents, we assume an *rc* model for the background current and calculate the parameters of that model in a region where we assume Na is not flowing. The full procedure uses an iteration method to check this assumption, but the method does not exclude the possibility that we are also subtracting a Na window current (see Methods). The equation for the background current is:

$$\langle i(t)\rangle = c[\mathrm{d}\langle V(t)\rangle/\mathrm{d}t] + g\langle V(t)\rangle + i_o.$$

Possible nonzero reversal potentials for the linear leak conductance, g, are lumped into the offset term, i_o. Fig. 2 illustrates the calculation of c, g, and i_o, outlined in detail in Methods. The left column shows an average action potential, $\langle V(t)\rangle$, and measured patch current, $\langle i(t)\rangle$. The measured current is the dark, noisy trace. The data are truncated to exclude the time when we expect Na current to flow using a two-step iteration. The averages are from simultaneous whole-cell/cell-attached patch records. The clear line through the current is the calculated error current, $i_E(t)$, from step *g* in Methods. The data in the right column repeats the procedure except that the traces are truncated to exclude the 250 ms after the upstroke. The parameters c, g, and i_o are identical for the two cases, from which we conclude that the subtracted currents are constant.

Fig. 3 illustrates the extrapolation of $i_E(t)$ into the time zone that we are certain contains the Na current. The smoother traces are the measured currents, and the darker, noisier traces with the higher peak values are the calculated currents using c, g, and i_o from Fig. 2. We determine these parameters individually for each V_p. The difference currents contain inward and outward components, noted in the center trace. Hyperpolarizing the patch by 20 mV ($V_p = 20$) increases the inward component and eliminates the outward component; depolarizing the patch by 20 mV ($V_p = -20$) decreases the inward component and increases the outward component. The current during the normal action potential would be the center trace $V_p = 0$.

Fig. 4 shows the difference currents from Fig. 3 normalized to their peak inward values. Note that depolarization shifts the peak of the inward current to the left, and that hyperpolarization shifts it to the right, consistent with standard models of the Na current (Mazzanti and DeFelice, 1987). To test for possible effects of perfusion by the whole-cell electrode, we did a series of experiments using a single cell-attached electrode. In such experiments the potential is unknown and it is impossible to correct for the background and capacitive current by the procedure illustrated in Figs. 1 and 2. Instead, in the single-electrode experiments, we subtracted the total patch current at $V_p = 0$ mV from the currents at $V_p = \pm$ 40 mV. This procedure gave the same qualitative results

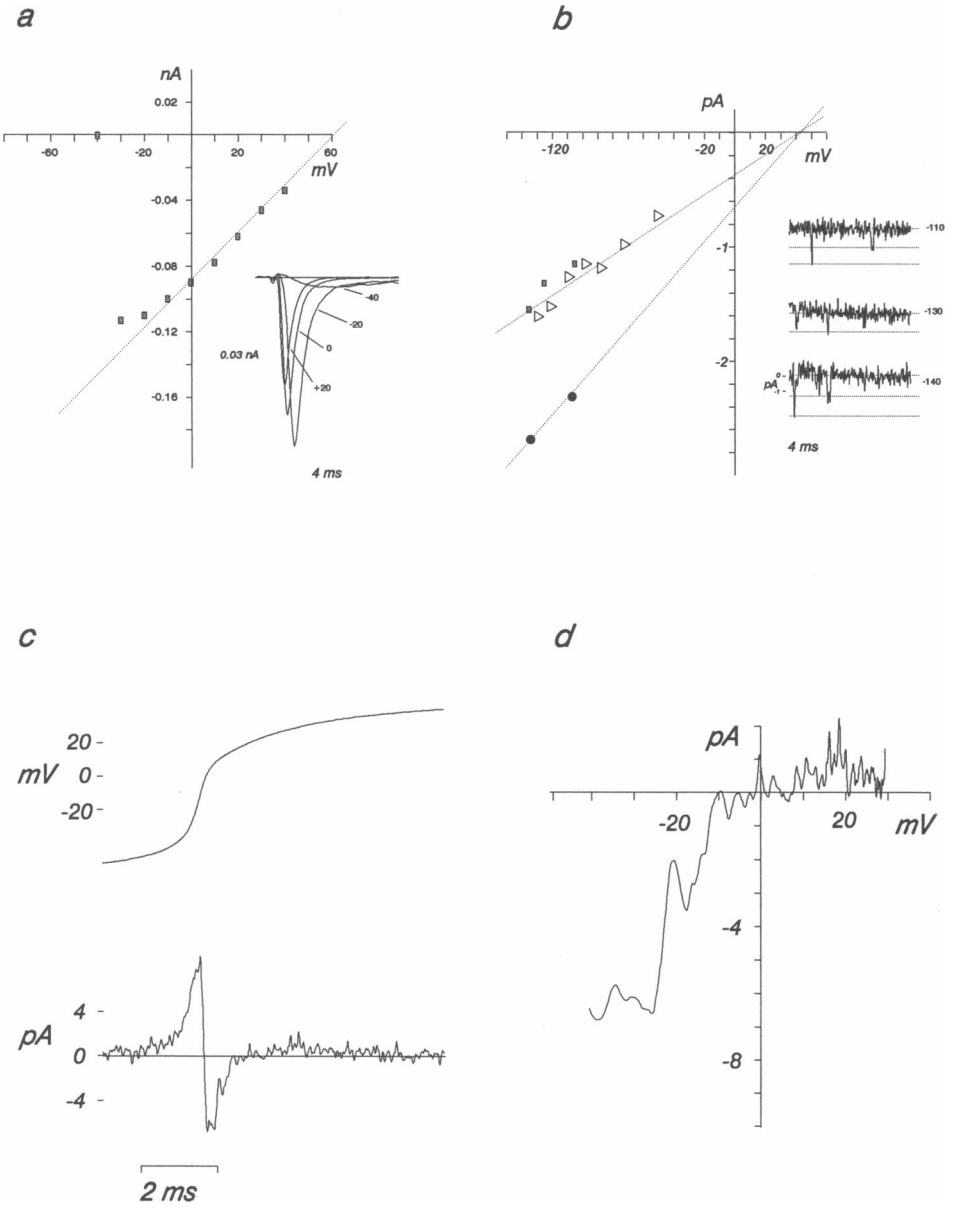

FIGURE 1 (*a*) Whole-cell, step-protocol voltage clamp of a single 7-d-old chick ventricle cell bathed in 120 mM Na, 10 mM TEA, and 3 mM Co (see Methods); this same solution was used in the patch pipette for the (*b*) cell-attached patch, step-protocol voltage clamp and the (*c*) cell-attached patch, AP-driven voltage clamp. In *a* the $I(V)$ curve is a plot of peak Na currents at various test potentials. The holding potential was -80 mV. The extrapolated reversal potential is ~ 60 mV. In *b* the $i(V)$ curves are the open-channel currents at various test potentials stepped from -80 mV. Solid squares and circles are from the experiment in the inset; the openings show at least two levels, and the slopes of the lines are 9 and 15 pS. The lower conductance is from pooled data from two experiments, one in which the openings were more frequent and the cell potential was estimated to be -50 mV, and the other in which the openings were less frequent (*inset*) and the cell potential was measured at -80 mV by breaking the patch after the experiment. The extrapolated reversal potential from these cell-attached patch experiments in nonbeating cells is ~ 40 mV. *c* is from a beating cell in which we record the voltage and patch current simultaneously. The top trace shows the leading edge of an action potential from the whole cell, and the bottom trace is the accompanying action current from the patch hyperpolarized by 20 mV to promote Na currents (see Methods and Mazzanti and DeFelice [1988] for details). The $i(V)$ curve in *d* is obtained by plotting the action potential against the action current directly. The $i(V)$ plot begins at ~ -40 mV at the foot of the action potential. The cell in *c* is in the normal bath solution containing 130 mM Na (see Methods). Unlike *a* and *b*, the $i(V)$ curve from the spontaneously beating cell in *d* is distorted by the capacitive transient which overlaps the Na current. This current, along with a leak current, must be removed before further analysis (see Methods and Fig. 2).

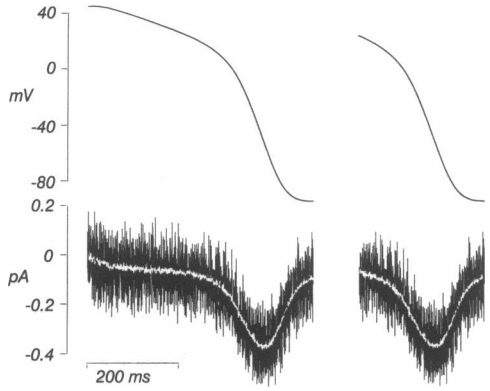

FIGURE 2 Calculation of the background and capacitive current from simultaneous recordings of whole-cell voltages and patch currents like those shown in Fig. 1 *c*, but focusing here not on the leading edge of the action potential but the falling phase. Trace in the top left corner is the average of 25 whole-cell action potentials; the noisy trace below it is an average of 25 patch action currents filtered at 5 kHz. The clear line through the data represents the calculated error current using data between upstroke +30 ms and maximum diastolic depolarization. Two curves in right column are the same except we used upstroke +250 ms. The calculated error current, $c(dV/dt) + gV + i_o$, is identical in both cases: with c = 0.318 pF, g = 0.5970 pS, and i_o = 0.0471 pA. We use these parameters, which are derived from the repolarization phase of the action potential, to eliminate the background currents during the rising phase (see Methods).

as the two-electrode experiment in Fig. 3 (see Methods for additional arguments).

Fig. 5 shows two tests we used to help identify the difference currents as Na currents. We integrated the currents to measure the relative amount carried by the inward and outward components. In these experiments we varied both the concentration of Na and the value of the potential in the pipette. At top, in 120 mM Na, all Na flows inward if we hyperpolarize the patch action potential by 20 mV ($V_p = -20$). At $V_p = 0$, when the patch action potential is the same as the cell action potential, 27% of the total Na flows outward. At bottom, the effect of changing Na while holding the pipette potential constant at 0 mV is depicted. The lower the Na in the patch, the higher the outward component relative to the inward component. For example, halving the concentration from 120 to 60 mM increases the number of Na ions that flow out of the patch from 27 to 61% of the number that flow inward. In 120 mM Na, near the normal value, we always find an outward current after the inward transient, however, the percentage varies widely and in one experiment it was 92%.

Fig. 6 plots the Na action current as a function of time (top) and voltage (bottom) during the action potential. In this experiment the reversal potential was 8.4 mV. It is difficult to determine the reversal potential or the percentage of outward current if the Na current is too small. Thus, we restricted the analysis to patches with at least 5 pA of inward peak current at $V_p = 0$. A virtually identical patch to the one in Fig. 5 gives a reversal potential of 15.3 mV. Lowering the Na in the pipette generally resulted in lower reversal potentials, but there was a poor correlation with the Nernst relationship if we assumed that internal Na was the same in the different cells. With 120 mM Na in the pipette, the dynamic reversal potential for the Na action current was never > 25 mV in any experiment.

Fig. 7 compares four experiments on Na current with a theoretical prediction (dark trace) based on the Ebihara and Johnson (1980) model. (The Hodgkin-Huxley model adjusted to our conditions gives similar results with a slightly better fit to the leading edge [Mazzanti and DeFelice, 1987].) We normalized the currents in the individual experiments to the inward peak and drove the model with the action potential of Fig. 2. The EJ equa-

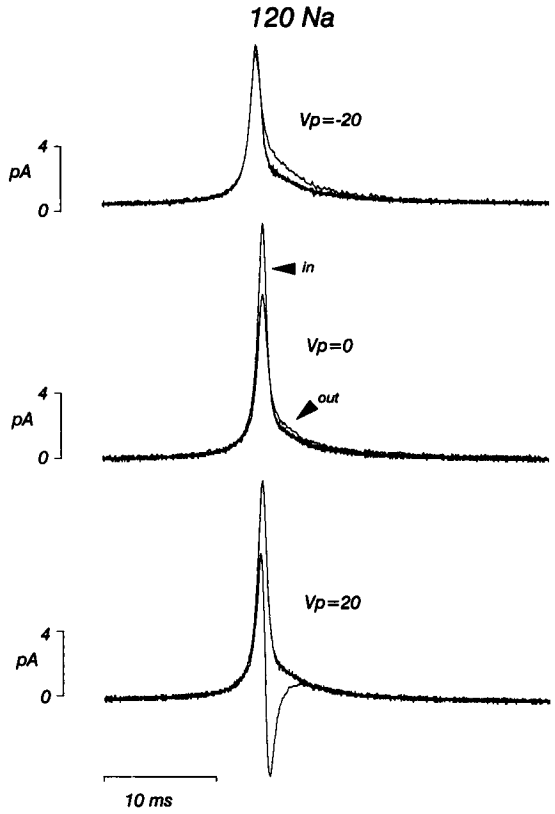

FIGURE 3 The effect of pipette potential (V_p) on the measured current (the lighter, smoother traces) and the error current. Each measured current is from an average of 36 traces digitized at a rate of 100 kHz and filtered at 5 kHz; each error current is calculated from c, g, and i_o, which were obtained by the method illustrated in Fig. 2. The measurement and the calculation are superimposed for each pipette potential. The center panel, $V_p = 0$, is from the experiment of Fig. 2. Top and bottom panels are from the same patch depolarized ($V_p = -20$) and hyperpolarized ($V_p = 20$) by 20 mV. Arrows in the center panel point to regions where subtraction of the two traces give inward and outward currents.

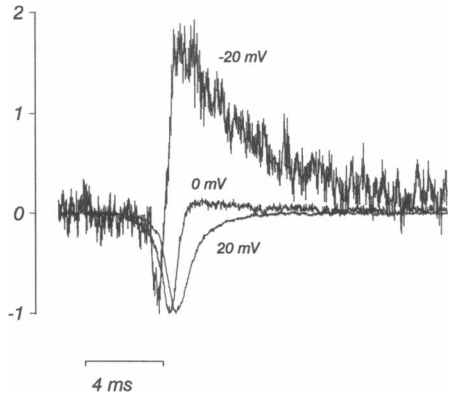

FIGURE 4 The difference currents obtained by subtracting error current from measured current in Fig. 3. The differences are normalized to the peak inward current to illustrate the relative sizes of the inward and outward components at each V_p.

tions were altered in the following way: we matched smooth functions to their data rather than use the discontinuous functions for α_h and β_h in the original paper, we used a nominal reversal potential of 10 mV, and we adjusted the rate constants to room temperature. Although the EJ model fails to reproduce the fast kinetics during the rising phase of the action potential, it gives the prolonged kinetics of the outward current.

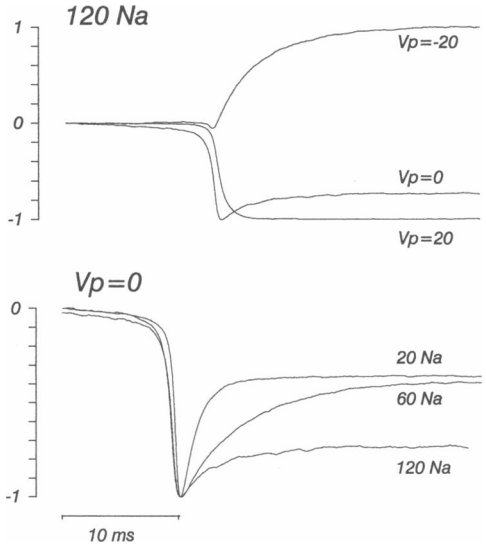

FIGURE 5 The integrals of the difference currents for various conditions in the patch. (*Top*) Na in the patch pipette is constant at 120 mM, and the potential is changed: $V_p = -20$, 0, and 20 mV. (*Bottom*) Potential in the patch pipette is constant at $V_p = 0$ mV, and the concentration of Na is changed: Na = 20, 60, and 120 mM. The integrals are normalized to their maximum inward or outward values.

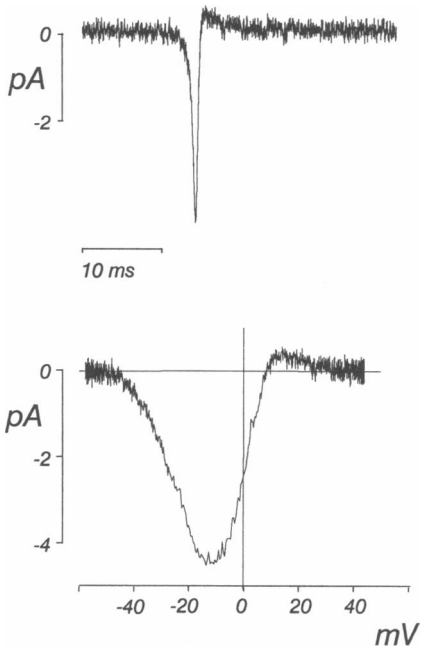

FIGURE 6 Na current during an action potential in normal external Na (120 mM) and normal bath potential (0 mV). Top trace is $i_{NA}(t)$ and bottom is $i_{NA}(V)$.

DISCUSSION

Previous papers have shown that models of the Na current based on step-protocol, voltage-clamp experiments describe the kinetics of the inward component of the action current reasonably well. Furthermore, the amplitude of the inward Na current gave acceptable values for channel density when they were compared with whole-cell recordings from the same tissue (Mazzanti and DeFelice, 1987; Fujii et al., 1988). The present experiments focus on the outward component of the Na action current.

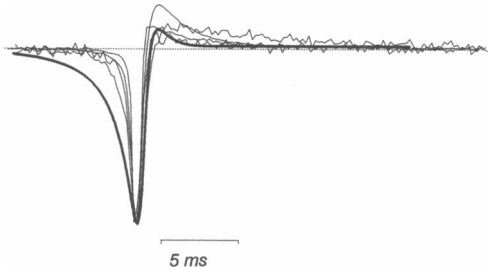

FIGURE 7 A comparison of measured Na action currents (the four lighter traces) with the Ebihara-Johnson model of the Na current, adjusted to room temperature and using a reversal potential of −10 mV. The data are from separate cells under the same conditions as Fig. 6.

Identification of this outward component as a Na current and not K, Ca, or some other current relies on the following arguments: (*a*) The outward component is probably not K because the patch solution contained TEA at concentrations that block K channels. More importantly, the delayed-rectifier and early-outward channels that are present in some experiments carry large, easily identified single-channel currents during the plateau (Mazzanti and DeFelice, 1988). Ca-activated K channels would also be far too large to miss. In the present study we rejected patches that contained these K-conducting channels. (*b*) The inward-rectifier carries no appreciable current in the plateau region, certainly not in 1.3 mM K (Mazzanti and DeFelice, 1988). (*c*) Ca channels cannot, in principle, conduct outward current during beating because the action potential never crosses the Ca reversal potential. In any case, the patch solution contained Co to block inward currents through Ca channels. Even if the Co in the patch blocks some of the Na current, it does not block it completely, and reducing the inward Na current in this way would not effect our interpretation. (*d*) Manipulation of pipette potential and pipette Na concentration changes the inward and outward components together and in a manner that is consistent with both components being a Na current. We think it is unlikely that the outward current is due to the Na/K pump, the Na/Ca exchanger, or to small unresolved channels that are not selective to Na, because the current responds quickly to voltage changes and because the gains in the outward direction are proportional to the losses in the inward direction. (*e*) Finally, models of the Na current, when driven by the action potentials we measure, give reasonable agreement with our experiments.

Na channels in cardiac tissue are capable of carrying an outward current, and they are selective for Na (Ebihara and Johnson, 1980; Follmer et al., 1987; Fozzard et al., 1987; Makielski et al., 1987; Sheets et al., 1987). The Na reversal potential in these nonbeating cells is always > 30 mV in Na concentrations that are comparable with ours. Under virtually identical conditions to the present study, except that the cells are not beating, the Na reversal potential is near 50 mV (Fujii et al., 1987), and our own experiments on nonbeating cells using single-channel or whole-cell data give 40–60 mV reversal potentials. The highest value we ever see in beating cells is 25 mV; in these cells the action potential overshoot and the early phase of the plateau potential can exceed 60 mV, hence there is a driving force for Na. The seemingly low values of the reversal potential in beating cells are probably not due to a build-up of Na in the omega figure of the patch, because similar patches in nonbeating cells give higher values close to those of the whole-cell recordings.

These data raise two questions: why is the Na reversal potential lower during beating, and what drives the action potential above the Na reversal potential? In answer to the first question, one interpretation would be that the Na concentration in beating cells is higher than in nonbeating cells. A reversal potential of 10 mV in 120 mM Na would imply an internal Na concentration of 80 mM, which far exceeds the measured free intracellular Na (13 mM) and perhaps even the total Na in our cells (McDonald and DeHaan, 1973; Fozzard and Sheu, 1980). It is possible, however, that the reversal potential of the Na action current reflects a local build-up of Na near the inner mouth of the Na channel through which a portion of the current returns to ground. For the second question, the only ion that could balance the outward Na current and drive the action potential above the Na reversal potential is Ca. This explanation would require that Ca channels start conducting within milliseconds of the peak of the inward Na current.

If our interpretation of the outward current in accurate, the cardiac action potential contains a repolarizing Na current that flows through the same channels that carry the depolarizing current. This Na repolarization, which would be in addition to the early outward and delayed-rectifier repolarization, lasts nearly 40 ms. Follmer et al. (1987) and Fozzard et al. (1987) report slowly decaying Na currents that would be consistent with the kinetics of the outward component we observe.

Although our data are from 7-d-old chick ventricle, the results may apply to later stages of development, including adult tissue, and to other species. Fujii et al. (1988) showed that in chick heart the principal change in Na conductance from 3 to 14 d is an increase in the number of virtually identical Na channels, and Sada et al. (1988) under conditions essentially similar to ours report that, except for channel density and reversal potential, Na conductance in 16–18-d-old chick heart is virtually identical to adult hearts, including mammalian species.

In the voltage-clamp experiments of Sada et al., the average Na reversal potential was 35 mV, using 10 mM Na in the whole-cell electrode and 140 Na in the bath. The Nernst potential for these conditions is 63 mV; Fozzard and Sheu (1980) predicted a reversal potential of 72 mV in similar circumstances. The low value in Sada et al. is probably not due to low Na selectivity, because in their experiments in 70 Na, the reversal potential shifted to 22 mV as expected from the Nernst equation. The explanation may be as follows: Sada et al. used both beating and nonbeating cells and interrupted the voltage-clamp protocols to monitor action potentials, with some cells firing spontaneously and others being stimulated. A clue to the measured 35 mV may lie in the wide range of values that Sada et al. report: the average was 35 mV but the range was 30–50 mV. Our results suggest that Na

loading during action potentials could have caused the low reversal potentials. Because it was not controlled, this variable could account for the wide range of reversal potentials. In their experiments and ours, it is probably the cell and not the whole-cell electrode that controls internal Na. If this interpretation is general, we should expect a broad range of E_{NA} in heart cells depending on the beat rate, and we would predict that the rapid repolarization phase of the cardiac action potential, which we believe is partly due to outward Na current, will be correlated with the Ca driving force.

We thank Ms. B. J. Cuti-Duke for preparing the tissue cultures and Mr. W. N. Goolsby for helping with the electronics and computer facilities necessary for this work.

This work was supported by the National Institutes of Health grant HL-27385.

Received for publication 19 August 1988 and in final form 21 August 1989.

REFERENCES

DeHaan, R. L. 1967. Regulation of spontaneous activity and growth of embryonic chick heart cells in tissue culture. *Dev. Biol.* 16:216–249.

Ebihara, L., and E. A. Johnson. 1980. Fast Na current in cardiac cells. *Biophys. J.* 32:779–790.

Follmer, C. H., R. E. Ten Eick, and J. Z. Yeh. 1987. Na current kinetics in cat atrial myocytes. *J. Physiol. (Lond.).* 384:169–197.

Fozzard, H. A., and S. S. Sheu. 1980. Intracellular K and Na activities of chick ventricle muscle during embryonic development. *J. Physiol. (Lond.).* 306:579–586.

Fozzard, H. A., D. A. Hanck, J. C. Makielski, B. E. Scanley, and M. F. Sheets. 1987. Na channels in cardiac Purkinje cells. *Experientia (Basel).* 43:1162–1168.

Fujii, S., R. K. Ayer, and R. L. DeHaan. 1988. Development of the fast Na current in early embryonic chick heart cells. *J. Membr. Biol.* 101:209–223.

Kell, M. J., and L. J. DeFelice. 1988. Surface charge in cardiac inward-rectifier channels measured from single-channel conductance. *J. Membr. Biol.* 102:1–10.

Makielski, J. C., M. F. Sheets, D. A. Hanck, C. T. January, and H. A. Fozzard. 1987. Na current in voltage clamped internally perfused canine cardiac Purkinje cells. *Biophys. J.* 52:1–11.

Mazzanti, M., and L. J. DeFelice. 1987. Na channel kinetics during the spontaneous heart beat in chick ventricle cells. *Biophys. J.* 52:95–100.

Mazzanti, M., and L. J. DeFelice. 1988. K channel kinetics during the spontaneous heart beat in chick ventricle cells. *Biophys. J.* 54:1139–1148.

McDonald, T. F., and R. L. DeHaan. 1973. Ion levels and membrane potential in chick heart tissue and cultured cells. *J. Gen. Physiol.* 61:89–109.

Patlak, J. B. 1988. Na channel subconductance levels measured with a new variance-mean analysis. *J. Gen. Physiol.* 92:413–430.

Sada, H., M. Kojima, and N. Sperelakis. 1988. Fast inward current properties of voltage-clamped cells of embryonic chick heart. *Am. J. Physiol.* 24:H540-H553.

Sakmann, B., and E. Neher. 1983. Single-Channel Recording. Plenum Publishing Corp., New York. 45.

Scanley, B. E., and H. A. Fozzard. 1987. Low conductance Na channels in canine cardiac Purkinje cells. *Biophys. J.* 52:489–495.

Sheets, M. F., B. E. Scanley, D. A. Hanck, J. C. Makielski, and H. A. Fozzard. 1987. Open Na channel properties of a single canine cardiac Purkinje cells. *Biophys. J.* 52:13–22.